

104 (1967).

¹³R. A. Day and H. R. Griem, *Phys. Rev.* **140**, A1129 (1965).

¹⁴A. C. Kolb and H. R. Griem, in *Atomic and Molecular Processes*, edited by D. R. Bates (Academic Press Inc., New York, 1962), Chap. 5.

¹⁵H. F. Berg, A. W. Ali, R. Lincke, and H. R. Griem, *Phys. Rev.* **125**, 199 (1962).

¹⁶H. R. Griem, *Plasma Spectroscopy* (McGraw-Hill

Book Co., New York, 1964).

¹⁷M. R. Null and W. W. Lozier, *J. Opt. Soc. Am.* **52**, 1156 (1962).

¹⁸J. T. Davis and J. M. Vaughan, *Astrophys. J.* **137**, 1302 (1963).

¹⁹H. F. Berg, W. Ervens, and B. Furch, *Z. Physik* **206**, 309 (1967).

²⁰J. R. Greig, C. P. Lim, G. A. Moo-Young, and G. Palumbo, *Bull. Am. Phys. Soc.* **13**, 265 (1967).

PHYSICAL REVIEW A

VOLUME 1, NUMBER 2

FEBRUARY 1970

Propagation of a Cavity-Dumped CO₂ Laser Pulse through SF₆

P. K. Cheo

Bell Telephone Laboratories, Whippany, New Jersey 07981

and

C. H. Wang*

Bell Telephone Laboratories, Holmdel, New Jersey 07733

(Received 8 July 1969; revised manuscript received 6 October 1969)

Coherent interactions between short CO₂ laser pulses and a resonant absorbing SF₆ gas medium have been examined carefully, using a laser cavity-dumped rectangular pulse with a width of 20 nsec and input intensities from 10 to 10⁴ W/cm². Parameters studied included the width, shape, and delay time of the transmitted pulse after propagation through several absorption lengths of SF₆ cell. In addition to these measurements, we have observed two new phenomena, namely, optical free induction decay and edge echo, which are induced by this short rectangular CO₂ laser input pulse. Results indicate that although level degeneracy in SF₆ may be involved, the simple two-level model can account qualitatively for most observed phenomena, with the exception that the observed shape of a 2π pulse deviates significantly from the symmetric hyperbolic-secant function predicted by the simple two-level theory. In the π pulse region, we have demonstrated that the free-induction-decay tail can be valuable for studies of atomic and molecular collision processes.

I. INTRODUCTION

Coherent interaction of a short laser pulse with a resonant medium is currently a subject of considerable interest. It was shown first by McCall and Hahn¹ that a ruby laser pulse of high intensity can propagate through an inhomogeneous absorbing medium (also ruby) without attenuation but with a delay in time. This phenomenon is known as self-induced transparency and has recently been studied in detail.² A similar effect has also been observed³ in SF₆ gas using 10.6-μ pulses from a CO₂ laser. In this paper, we report the observation in SF₆ of an optical free induction decay and an edge echo on an initial short 20-nsec rectangular 10.6-μ P(20) CO₂ laser pulse using the cavity-dumping technique.⁴ Similar phenomena with pulses from the P(18) and P(22) CO₂ transitions were also observed. For a simple model consist-

ing of two nondegenerate quantum states with an inhomogeneously broadened line, theory² shows that the stable condition of self-transparency results after the initial pulse traversing through a few absorption lengths into the resonant medium and the pulse evolves into a symmetric hyperbolic-secant pulse in time and space with a pulse area corresponding to a "2π pulse." More recently, numerical computations have also been made⁵ with the emphasis on the evolution of a pulse as it develops into a 2π pulse. However, there exist differences in interpretation^{2,5-7} of previous experiments^{3,7} which were performed using a rotating mirror Q-switched CO₂ laser pulse.⁸ By using a short and flat-topped CO₂ laser pulse, we have been able to examine in detail the dynamic evolution of this input pulse through an optically thin as well as thick SF₆ absorbing medium. This was accomplished by studies of the pulse shape, pulse

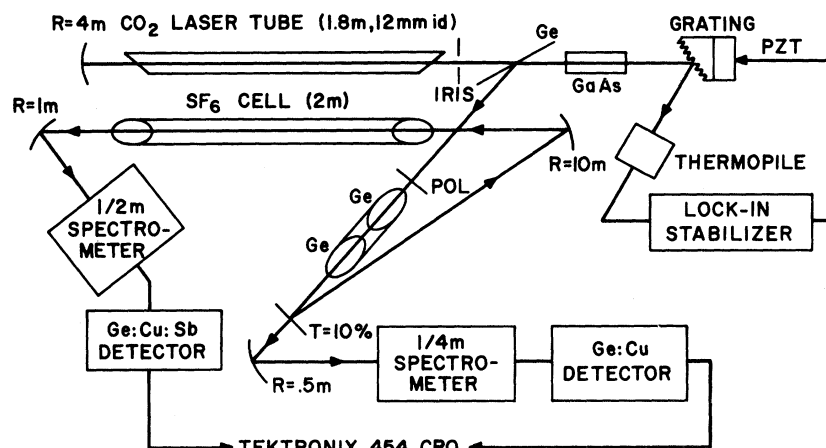


FIG. 1. Experimental arrangement.

delay time⁹ τ_D , pulse width¹⁰ τ_w , and output-pulse intensity I_S , as functions of SF_6 pressure and the input-pulse intensity I_0 varying from 10 – 10^4 W/cm^2 . Results can readily be compared with existing theories. The effect of helium on the free-induction-decay tail was also investigated.

II. EXPERIMENTAL PROCEDURE

The experimental arrangement is shown in Fig. 1. Our measurements were made with a short ~ 20 -nsec rectangular CO_2 laser pulse [see Fig. 3(a)] as the input to a 2-m-long SF_6 absorption cell. The pulse was dumped out from the laser cavity by means of intracavity GaAs electro-optic Q -switching technique.⁴ Oscillation was maintained on a single rotational line of the (001)-(100) CO_2 vibrational transition by means of a diffraction-grating cavity mirror, and the transverse intensity profile was Gaussian. The beam spot was collimated to ~ 4 mm in diam along the entire length of the SF_6 absorption cell with a spherical mirror of 10-m radius. The laser pulse was linearly polarized, and its input intensity I_0 could be continuously varied over a wide range, from 10 – 10^4 W/cm^2 , with a combination of two polarizers. I_0 was monitored near the entrance of the SF_6 cell with a beam splitter, a monochromator, and a Cu-doped Ge photoconductor cooled to $4^\circ K$. The output signals from the SF_6 cell, shown in Fig. 3(b)–3(h), were detected by a fast Ge:Cu (Sb) photodetector cooled at liquid helium temperature and a Tektronix 454 oscilloscope. In front of this detector, a monochromator was also used to insure that the observed output pulse had the same wavelength as the input pulse. The combined response time of the detector and oscilloscope was $\lesssim 4$ nsec.

III. RESULTS AND DISCUSSION

The measurements of the absolute output-pulse intensity I_S versus the absolute input-pulse inten-

sity I_0 over the range from 5 to 10^4 W/cm^2 are shown in Fig. 2. Data were obtained in a 2-m-long SF_6 absorption cell at 20, 30, 50, and 70 mTorr of SF_6 pressure. Since the shape of the output pulse varies as a function of I_0 , as shown in Fig. 3, this has been accounted for in the measurements of I_S . The calibration of the absolute peak power was made in both high (> 100 W/cm^2)

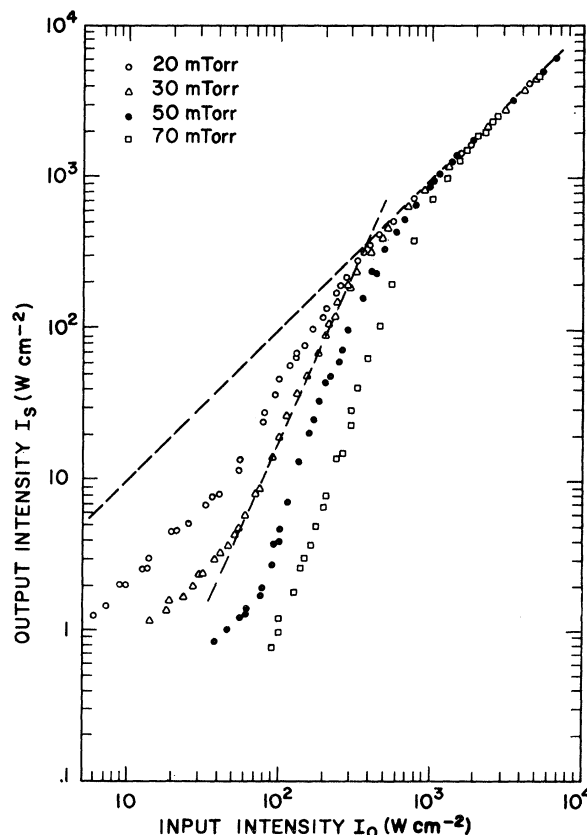


FIG. 2. Output- versus input-pulse intensities at 10.6μ through a 2-m-long SF_6 cell.

and low ($< 100 \text{ W/cm}^2$) power-density regions. Care was taken to assure that the detectors were not saturated. Even though the accuracy of the absolute power calibration can be as large as $\pm 20\%$, the relative correspondence between the input and output intensities was limited only by the readouts from the dual-beam oscilloscope traces to about a few percent. The error in absolute calibration should not change the shape of the curves but may cause a shift of all curves; thus, it has an effect on the threshold values. Two points are worth noting: (i) Threshold value I_{th} for complete self-induced transparency, which is obtained by the intersection of two straight lines (as shown in Fig. 2), is relatively constant ($I_{\text{th}} \lesssim 500 \text{ W/cm}^2$) for 20-, 30- and 50-mTorr SF₆ pressures; and (ii) the transition region, in which the values of I_s depart from linear absorption and increase rapidly to complete transparency ($I_s = I_0$), occurs in a narrow input-intensity range ($50 \lesssim I_0 \lesssim 1000 \text{ W/cm}^2$), for SF₆ pressures ranging from 20 to 50 mTorr. As an example, at 50-mTorr SF₆ pressure, I_s/I_0

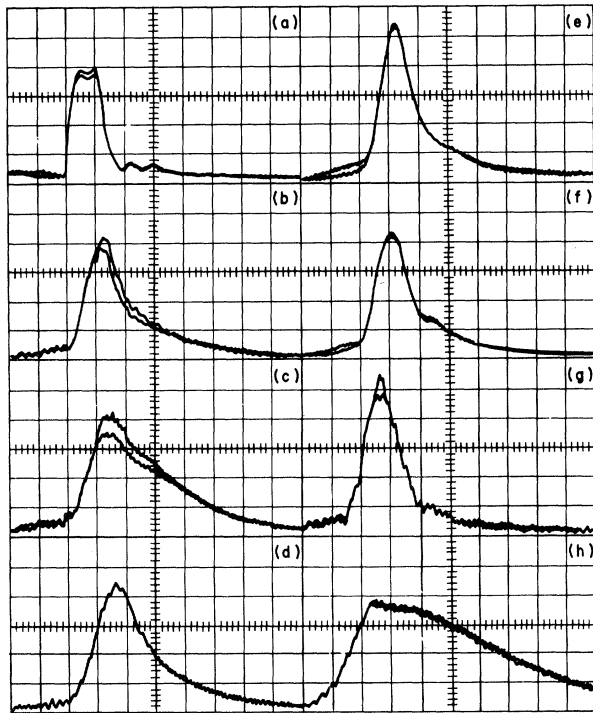


FIG. 3. The evolution of a flat-topped CO₂ laser pulse of 20-nsec duration through a 2-m-long SF₆ absorption cell. The horizontal scale for all traces is 20 nsec/cm: (a) $P_{\text{SF}_6} = 0 \text{ mTorr}$; (b) $P_{\text{SF}_6} = 20 \text{ mTorr}$ and $I_0 = 26 \text{ W/cm}^2$; (c) $P_{\text{SF}_6} = 50 \text{ mTorr}$ and $I_0 = 94 \text{ W/cm}^2$; (d) $P_{\text{SF}_6} = 50 \text{ mTorr}$ and $I_0 = 180 \text{ W/cm}^2$; (e) $P_{\text{SF}_6} = 50 \text{ mTorr}$ and $I_0 = 690 \text{ W/cm}^2$; (f) $P_{\text{SF}_6} = 50 \text{ mTorr}$ and $I_0 = 1470 \text{ W/cm}^2$; (g) $P_{\text{SF}_6} = 50 \text{ mTorr}$, $P_{\text{He}} = 2 \text{ Torr}$, and $I_0 = 113 \text{ W/cm}^2$; and (h) $P_{\text{SF}_6} = 70 \text{ mTorr}$ and $I_0 = 113 \text{ W/cm}^2$.

changes from 0.017 to 1 as I_0 changes from 100 to 900 W/cm^2 . This differs from that obtained previously³ with rotating-mirror Q-switched CO₂ laser pulses.

Figure 3 shows the change of pulse shape from an initially flat-topped input pulse propagating through a SF₆ cell as a function of input-pulse intensity. It is clear from Fig. 3(b)–3(h) that the output pulse is distorted in shape and always has a longer tail than the 6-nsec fall time of the input pulse shown in Fig. 3(a). Furthermore, the fact that the rise time of the output pulse is not sensitive to gas pressure or the input intensity suggests that the leading portion of the output pulse is mainly due to the transmission of the input pulse as it propagates along the SF₆ cell. More strikingly, one observes that the shape and decay time associated with the trailing portion of the pulse change dramatically as the input-pulse intensity or the gas pressure is varied. We attribute the trailing tail to a phenomenon which is an optical analog of free induction decay in an inhomogeneous magnetic field.¹¹ It is caused by radiation from induced dipoles undergoing free precession. For an optically thin and slightly inhomogeneous medium, the free induction decay can often be characterized by an inhomogeneous (reversible) decay time,¹² T_2^* , because the induced dipoles oscillate at different natural frequencies within the Doppler-broadened line. Therefore, the envelope of the free induction decay is proportional to the Fourier transform of the Doppler frequency distribution of the induced dipoles. However, for a very inhomogeneous medium, the formation of a free induction decay is somewhat different. Considering the case that T_2^* of an inhomogeneous broadened line is shorter than the input-pulse width τ_0 , one finds that molecules distributed within the Doppler profile do not respond uniformly to the frequency components associated with the input pulse. As a result, the output free-decay signal depends not on the width of the Doppler profile but on the shape and intensity of the input laser pulses; namely, a strong and short laser pulse will give a short free decay and a weak and long pulse will have a long decay.¹¹

In case of an optically dense resonant medium, the effect of propagation on the pulse shape is also important. For $T_2 \gg \tau_\omega$ (where T_2 is the phase-memory relaxation time) and for a nondegenerate two-level system, the propagation effect can be described in part by an equation for the pulse angle,^{1,2} θ given by

$$\frac{d\theta}{dz} = -\frac{1}{2}\alpha \sin\theta, \quad (1)$$

where α is the absorption coefficient of the medium, and is $0.35 \text{ cm}^{-1} \text{ Torr}^{-1}$ for SF₆ at the $P(20)$ 10.6- μ line. In Fig. 3(b), the free-induction-

decay signal is obtained from the cell filled with 20 mTorr of SF_6 pressure. At this pressure, the phase relaxation by molecular collision is negligible, and the solution of Eq. (1) gives $\theta_s = 0.26\pi$ at $Z = 2$ m for the initial pulse angle¹³ $\theta_0 = 0.46\pi$. Qualitatively, one thus expects the output-pulse width to be increased by a factor $(\theta_s/\theta_0)(I_0/I_s)^{1/2}$. Substituting the measured and calculated numbers, one finds that the free-decay pulse for Fig. 3(b) is broadened due to propagation effect only by a factor of 1.2. The measured full width at half-maximum intensity is 28 nsec, as opposed to 20 nsec for the input pulse. As discussed above, this free-decay width is expected from an inhomogeneously broadened line, because the Doppler width of SF_6 is about 30 MHz at $10.6\text{-}\mu$; and it corresponds to a T_2^* of about 9 nsec, which is about a factor of 2 smaller than the input-pulse width. In passing, it should be pointed out that while photon echoes in SF_6 have been observed¹⁴ with two rotating-mirror Q -switched CO_2 laser pulses, direct observation of the free induction decay with a rotating-mirror Q -switched pulse has not been possible because the minimum input-pulse width is too long (>200 nsec).

From Fig. 3(e), we see that as I_0 reaches the complete transparency region, the output pulses excluding the long tail become a symmetric bell-shaped function. In Fig. 4, we showed the detailed comparison between the experimental pulse shape and the theoretical shape $[I_0 \propto \text{sech}^2(t/\tau_\omega)]$ predicted by McCall and Hahn² on the basis of a two-level system. The experimental self-induced transparency pulse is somewhat steeper than the ideal $\text{sech}^2(t/\tau_\omega)$ pulse shape. It is likely that the

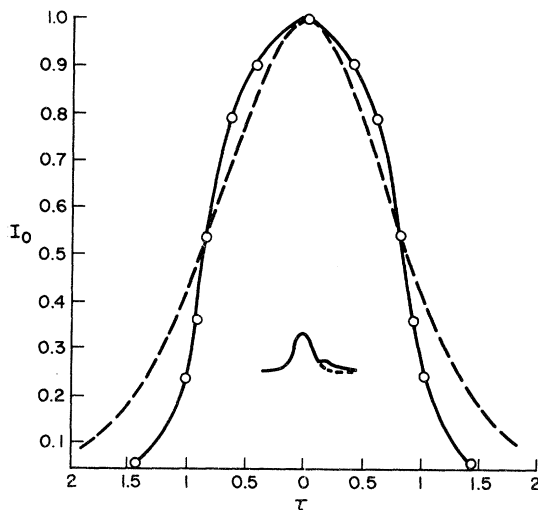


FIG. 4. The comparison of the experimental and the theoretical self-induced transparency pulse shapes. The smooth line and the broken line indicate the experimental and the theoretical pulse shapes, respectively.

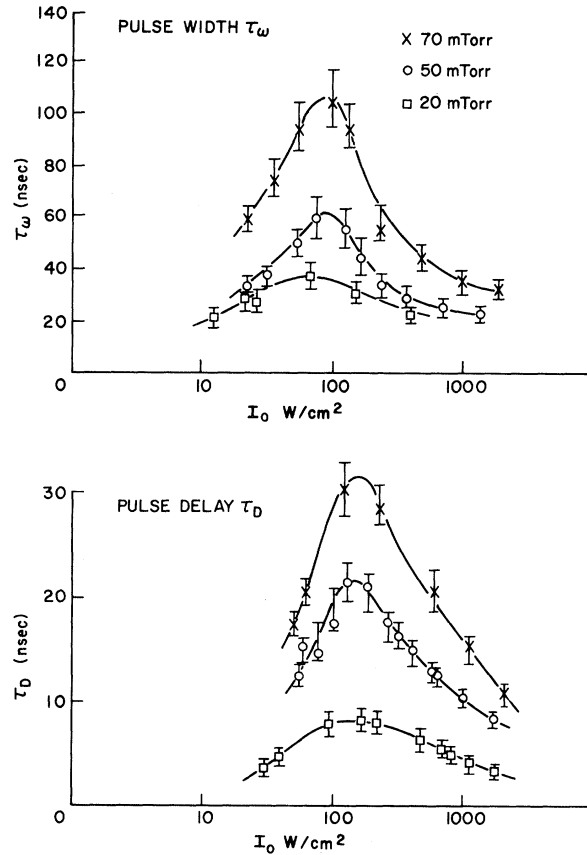


FIG. 5. The output pulse with τ_ω and the delay time τ_D between the input and output pulses versus input intensity I_0 .

deviation is due to the participation of the absorbing lines of high angular momentum states in SF_6 .^{7,15}

It may be noted in Fig. 3(f) that a small peak appears at the trailing portion of the output pulse. It needs to be pointed out that the small peak occurs at the input intensity corresponding to pulse angles θ less than 2.3π , and is, therefore, not due to the splitting pulse phenomenon.² The intensity and the shape of the small pulse vary with I_0 , but its position is centered about 40 nsec following the leading edge of the output pulse. This result suggests that the small peak is an optical analog of edge echo also commonly observed in NMR when an intense rectangular radio-frequency pulse is suddenly applied to a medium in a very inhomogeneous magnetic field.¹¹ Further, experimental studies of this phenomenon and the effects of pulse propagation on the detailed shape of free-induction-decay tail and edge echo are presently in progress.

The dependence of τ_ω and τ_D on I_0 for pulse propagation through the 2-m long absorption cell is shown in Fig. 5. Experimentally, we found

that local maxima in τ_ω and τ_D exist at I_0 values in the transition region. τ_ω and τ_D also increase with increasing SF₆ pressure for all values of I_0 . At low SF₆ pressure, the threshold I_{th} for nearly complete transparency is about 4 times the values of I_0 at maximum τ_D , indicating that the intensity for maximum τ_D corresponds to the case of a π pulse. Similar conclusions have been reached by Hopf and Scully⁵ in their theoretical investigation of π pulse propagation through a resonant medium. From the computer calculation, they⁵ proposed an expression for τ_D in the case of a π pulse as $\tau_D = \frac{1}{2}\tau_0 e^{\alpha L/2}$, whereas for a 2π pulse,² $\tau_D = \frac{1}{2}\tau_0 \alpha L$. The results of Ref. 5 yield τ_D versus I_0 curves which are similar in shape to Fig. 5. However, the computed value of τ_D for the case of SF₆ is about a factor of 3 larger than our measured value. The fact that τ_D has a maximum for a π pulse implies that there must exist a local maximum for τ_ω . This can be understood from the following simple argument: $\theta = \pi$ is a solution of Eq. (1) even though it is an unstable one. If there are no other perturbations to affect the value of θ , this π pulse should propagate without change in pulse angle. Therefore, as the pulse energy is transferred to the medium, the pulse width must be broadened in order to conserve the pulse angle. For a pulse angle greater or smaller than π , the pulse-broadening effect will not be as large, because, according to Eq. (1), the pulse angle will evolve into a 2π or a zero π pulse.

We also investigated the effects of a foreign gas on the pulse shape. The output-pulse shape for a mixture of 50 mTorr of SF₆ and 2 Torr of He is shown in Fig. 3(g). Results show that the pulse width is considerably narrower than that of the pure SF₆ case, see Fig. 3(c). We have measured the exponential decay-time constant τ_e of the output pulse over a time period covering more than a 60% drop from the peak intensity value as a function of He pressure from 0 to 2 Torr. The value of $(\tau_e)^{-1}$ increases from $2.2 \times 10^7 \text{ sec}^{-1}$ at $P_{He} = 0$

Torr to $7.6 \times 10^7 \text{ sec}^{-1}$ at $P_{He} = 2$ Torr. This is expected because collisions between SF₆ and He tend to destroy the phase memory and shorten T_2 . The pulse-narrowing effect is most pronounced at the input-pulse intensity for maximum pulse width. From the measured $(\tau_e)^{-1}$ versus P_{He} curve, we obtain the relaxation cross section¹⁶ σ to be $5.9 \times 10^{-15} \text{ cm}^2$. This value is in a fairly good agreement¹⁷ with that obtained from the photon-echo experiment,¹⁴ but disagrees with that obtained from the self-induced transparency experiment reported in Ref. 3.

Since the attenuation of the photon-echo intensity due to the collision damping occurs mostly in the absence of field, namely, in time between pulses, the fact that our measured cross section agrees with the photon-echo measurement is significant. It serves as an additional support for our interpretation of the trailing portion of the output pulses as free-induction-decay trail, broadened by the propagation effect.

IV. CONCLUSION

Free induction decay and an edge echo have been observed by pulsed irradiation in SF₆ at 10.6 wavelength. Studies of pulse width, pulse-delay time, and pulse intensity with a short rectangular CO₂ laser input pulse provide a better understanding of the behavior of an optical pulse propagating through an inhomogeneously broadened resonant medium and bring the theoretical^{2,5} and experimental studies to a more unified ground. We have also demonstrated that studies of pulse shape in π pulse region can yield quantitative information regarding atomic and molecular collisional processes.

ACKNOWLEDGMENTS

We are grateful to J. P. Gordon for his critical reading of the manuscript and to R. P. Reeves for technical assistance.

*Present address: Department of Chemistry, University of Utah, Salt Lake City, Utah 84112.

¹S. L. McCall and E. L. Hahn, Phys. Rev. Letters **18**, 908 (1967).

²S. L. McCall and E. L. Hahn, Phys. Rev. **183**, 457 (1969).

³C. K. N. Patel and R. E. Slusher, Phys. Rev. Letters **19**, 1019 (1967).

⁴T. J. Bridges and P. K. Cheo, Appl. Phys. Letters **14**, 262 (1969).

⁵F. A. Hopf and M. O. Scully, Phys. Rev. (to be published).

⁶C. K. Rhodes, A. Szoke, and A. Javan, Phys. Rev. Letters **16**, 1151 (1968).

⁷C. K. Rhodes and A. Szoke, Phys. Rev. (to be published).

lished).

⁸A typical rotating Q-switched CO₂ laser pulse has an asymmetric bell shape and a full width at half-maximum intensity 0.2 to 1 μsec .

⁹The delay time τ_D is defined as the time difference between the peak of the output pulse and the center-of-the-square top input pulse.

¹⁰The pulse width τ_ω is defined as full width at half-maximum intensity.

¹¹Arnold Bloom, Phys. Rev. **98**, 1105 (1955).

¹²The inhomogeneous dephase time T_2^* is defined as $T_2^* = (4 \ln 2)^{1/2} / 2\pi \Delta D$, where ΔD is the Doppler width.

¹³The value $\theta_0 = 0.46\pi$ is extrapolated from the measured I_S versus I_0 data, as shown in Fig. 2, for $P_{SF_6} = 20$ mTorr by assuming $\theta_0 = 2\pi$, when $I_S = I_0$. The measured I_0 for

$\theta_0 = 2\pi$ is about 500 W/cm^2 . The measured I_0 and I_S for $\theta_0 = 0.46\pi$ are 26 and 6 W/cm^2 , respectively.

¹⁴C. K. N. Patel and R. E. Slusher, *Phys. Rev. Letters* **20**, 1087 (1968).

¹⁵R. L. Abrams and A. Dienes, *Appl. Phys. Letters* **14**, 237 (1969).

¹⁶ $\sigma = k/n \langle v \rangle$, where k is the slope of the linear plot and $\langle v \rangle$ the average thermal velocity of the SF_6 gas.

¹⁷In Ref. 14, σ was defined differently from ours by a factor of 2π . The cross section obtained in Ref. 14 is $1.2 \times 10^{-15} \text{ cm}^2$.

Ni $L\alpha$ Self-Absorption Spectrum*†

D. Chopra

Physics Department, East Texas State University, Commerce, Texas 75428

(Received 18 July 1969)

The shape and position of the Ni $L\alpha$ x-ray emission line ($\lambda = 14.53 \text{ \AA}$) has been studied as a function of bombarding electron energy ranging from 2 to 30 keV. The bombarding electrons struck the anode at normal incidence, and x rays were viewed by the spectrometer at a 90° takeoff angle. The Ni $L\alpha$ lines recorded under these conditions exhibit an increasing attenuation of intensity on the high-energy side and a shifting of the peak position towards lower energy with increasing bombarding electron energy. These changes are interpreted as due to differential self-absorption of the emission line in the anode. The emission measurements have been used to obtain the "L self-absorption spectrum" of Ni, which agrees favorably with the absorption spectrum reported in the literature.

INTRODUCTION

The Ni $L\alpha$ x-ray emission line represents the transitions of valence band ($M_{IV,V}$) electrons to vacancies in the L_{III} shells of Ni atoms. It is believed by some authors that if the combined width of the Ni L_{III} states and the spectral-window function of the instrument which records the spectrum is small compared with the width of the Ni valence band, one can learn from the shape of the observed Ni $L\alpha$ line the density of filled valence states in Ni. For purposes of gaining such information, various authors¹⁻¹¹ have recorded the Ni $L\alpha$ line. It is a significant fact that almost no agreement exists regarding the detailed features of the line and of the location of its peak position. The differing experimental results and the attempted explanations of various authors suggested that a systematic experimental investigation of the Ni $L\alpha$ emission line as a function of bombarding electron energy ranging from 2 to 30 keV might clarify the unsettled points in the interpretation of x-ray spectra. As a result of the present study, it has been found that the changes in the shape and position of the Ni $L\alpha$ line are related to the self-absorption of radiation by the material of the anode.

EXPERIMENTAL

The data on the Ni $L\alpha$ x-ray emission line spectra were recorded with the two-crystal vacuum x-ray spectrometer at New Mexico State University. Potassium acid phthalate (KAP) crystals ($2d = 26.6 \text{ kxu}$) were used as diffracting elements, which were grown from a supersaturated water solution in this laboratory. The excellent spectrometric properties of KAP crystals for the wavelength range of the present investigation have already been established.¹²

The spectral window, implied by the width of the $(1, -1)$ curve at the Ni $L\alpha$ wavelength, is $\approx 0.6 \text{ eV}$ (resolving power $\lambda/d\lambda \sim 3000$), which is good enough to reproduce satisfactorily the structure on the high-energy side of the Ni $L\alpha$ line previously reported. The data were obtained by the operation of the two-crystal spectrometer in a double-rotation tracking mode.¹³ The term "double" implies that both crystals are rotated for scanning the spectrum, as compared to the rotation of the first (central) crystal only in the case of the single-rotation mode. In the method of double rotation, x rays which pass through the instrument originate from the same region of the anode, strike the same